BİTLİS EREN ÜNİVERSİTESİ
FEN BİLİMLERİ DERGİSİ

ISSN: 2147-3129 / e-ISSN: 2147-3188

Article Type : Research Article
Received : March 12, 2025
Revised : April 11, 2025
Accepted : April 15, 2025
DOI : 10.17798/bitlisfen.1656421

Year : 2025
Volume : 14
Issue : 2
Pages : 1182-1195

EFFECT OF INTERFACE STRENGTH ON ELASTIC AND TOUGHNESS PROPERTIES OF GRAPHENE-REINFORCED SI3N4 NANOCOMPOSITES

Betül ASLAN [1], **Osman BAYRAK [1,*]**

[1] *Gazi University, Mechanical Engineering Department, Ankara, Türkiye*

[2] *Bursa Technical University, Mechanical Engineering Department, Bursa, Türkiye*

**** Corresponding Author:*** *osman.bayrak@btu.edu.tr*

ABSTRACT

Silicon nitride is used in advanced engineering applications. Its toughness can be improved when they are reinforced with nanoparticles, such as graphene. Although toughness improvement is relatively more achievable with the reinforcement, elastic properties of nanocomposites are generally inferior to those of monolithic ceramics. Experimental works give rich insight into the mechanical characteristics of graphene-Si3N4 nanocomposites. However, there is no consensus yet in literature on why Young's modulus decreases upon addition of graphene into Si3N4 nanocomposites. In this study, we aimed to reveal the reason behind the deterioration of the Young's modulus. We created and verified finite element models based on the microstructural and mechanical data provided in literature. Different void and interfacial interaction properties were tested on the models. Results revealed that graphene does not act like voids within the matrix. It rather induces randomly dispersed porosities within the interfaces. Toughness of nanocomposites improved with increase of interfacial strength. However, interfacial strength did not directly affect Young's modulus of nanocomposites. Following the inducing of porosities within the interfaces in finite element models, it was observed that secant modulus decreased. This finding implies that optimizing porosity distribution via contact discontinuities can help achieve approximating elastic properties of graphene-Si3N4 nanocomposite models. Findings of this study will contribute to future research on nanocomposites, including fracture behavior modeling, and toughness mechanisms.

Keywords: Graphene, Si3N4, Mechanical properties, Microstructure, Finite element modeling, Interface.

1 INTRODUCTION

Ceramics are employed in special application fields of engineering [1], [2] due to their physical properties that are not provided by metals and polymers. However, they come with a well-known drawback, which is brittleness. One of the commonly applied processes to reduce the brittle characteristic of ceramic materials is to reinforce them with nanofillers [3]. Among ceramic materials, silicon nitride (Si_3N_4) has been studied widely by researchers who work on ceramic-matrix composites [4]. Si_3N_4 has got remarkable properties such as high thermal shock resistance, high-temperature resistance, chemical stability, good wear resistance, corrosion resistance, and outstanding mechanical strength [5].

Graphene has emerged as a candidate filler for reinforcing ceramics [6] as well as polymers [7] and metals [8]. Graphene is a one-atom-thick two-dimensional (2D) allotrope of carbon [9]. It has superior mechanical [10] and electrical properties [11], and its surface area/volume ratio is very large [12], making it a good candidate for ceramic-matrix composites. In recent years, studies have shown that the addition of graphene into ceramic materials can improve properties of the material such as electrical conductivity and fracture toughness [13]. While toughness improvement is achieved [14], some other mechanical properties of ceramics, like Young's modulus and bending strength, are affected adversely upon incorporation of graphene into Si_3N_4 ceramics [3], [15].

Kun et al. [16] observed a homogeneous distribution of graphene nanoplatelets but with surrounding porosities. In all cases of different graphene types, nanocomposites with lower concentrations (1 wt%) of the nanoplatelets exhibited better mechanical performance compared to the ones with higher concentrations (3 wt%). Combined with the finding of porosity phenomenon in all nanocomposites cases, it was concluded that the higher concentration of the nanoplatetlets introduced higher degrees of porosity within the nanocomposites, eventually leading to the deteriorated mechanical properties. Senier et al. [17] observed a decrease in Young's modulus of the nanocomposites compared to monolithic Si_3N_4 ceramics. They attributed the decrease to that graphene nanoplatelets acted as voids within the matrice. Michalkova et al. [18] showed that nanocomposites had agglomerated nanoplatelets but with varying degrees of voids. They revealed that adding a relatively high density of graphene (7 wt%) lead to unavoidable agglomerations hence the deterioration of mechanical properties of the nanocomposites. Study by Rutkowski et al [19] also support this finding. Senier et al. [15] showed that 3 wt% graphene-reinforced nanocomposites had a lower Young's modulus of 308

GPa compared to that of monolithic ceramic, which is 324 GPa. They attributed the decrease to wavy interfaces. Cygan et al. [20] reported that while toughness improvement is achievable with addition of graphene, hardness and Young's modulus almost always decrease. The highest Young's modulus obtained for monolithic Si_3N_4 was calculated as 324 GPa at a sintering temperature of 1650 °C. Under the same sintering conditions, it was ~282 GPa for nanocomposites. Balazsi et al. [21] showed that beyond 5 wt% graphene addition, wear properties of Si_3N_4 nanocomposites improved. However, hardness of the nanocomposites decreases with 3 wt% and beyond. While Vickers hardness (HV) of monolithic Si_3N_4 was ~17 GPa, it was determined as ~16.2 GPa for 3 wt% graphene-reinforced nanocomposites. Zhang et al. [22] denoted weak bonding between graphene and the ceramic matrix and studied effect of orientation on the crack deflection characteristics. They reported an increase in toughness (6.3 $MPa \cdot m^{1/2}$ to 8.7 $MPa \cdot m^{1/2}$) and a decrease in hardness (14.5 GPA to 13.9 GPa) with addition of 1 wt% graphene, with which the best mechanical performance among the nanocomposites were obtained. Tapasztó et al. [23] showed that toughness improvement is higher with thinner graphene nanoplatelets. However, reduction in hardness (HV, 17.5 GPa to 13.7 GPa) could not be avoided with thinner graphene. Also, nanocomposites with 3 wt% thin graphene nanoplatelets exhibited substentially higher toughness (5.1 $MPa \cdot m^{1/2}$ to 10.5 $MPa \cdot m^{1/2}$). Bódis et al. [24] showed that an improvement in toughness without a compromised Young's modulus can be achieved for 1 wt% graphene addition. However, at 3 wt% and beyond, a signifacant decrease in Young's modulus was reported.

Almost all experimental studies on graphene-reinforced Si_3N_4-matrix nanocomposites, as mentioned above [15], [17], [19], [22], [23], [24], argues the anisotropic characteristics of their mechanical properties. The anisotropy is introduced by orientation distribution of nanoplatelets in nanocomposites [19], [22], [25]. Beyond 1 wt% of graphene addition, Young's modulus decreases while toughness is improved [3], [13], [15], [19], [22], [23], [24]. As can be seen in literature [16], [26], nanocomposites up to 3 wt% graphene show a homogeneous dispersion characteristic. Above this weight fraction, unavoidable agglomerations are often observed [18], [19]. As discussed above, literature presents effects of graphene on mechanical performance of Si_3N_4-matrix nanocomposites through experimenting wide range of manufacturing methods. However, there is no consensus on what causes the decrease in elastic and hardness properties of the nanocomposites while toughness improvement is achieved. While some studies argue that graphene acts as voids [17], [19], others put forward the porosities that sits in the interfaces [16], [18], [22], [24]. This ambiguity is more pronounced

with 3 wt% graphene ratio, beyond which other microstructural issues come into place, such as non-homogenous distribution as discussed above. Therefore, void and/or porosity effect becomes relatively more dominant with 3 wt% graphene concentration in Si_3N_4, making this concentration a good option to analyze the aforementioned phenomenon. Our aim is to disclose whether graphene act as voids and/or cause compromised interfacial strength due to interfacial porosities. In order to reach our aim, we create finite element models of graphene-reinforced Si_3N_4 nanocomposites based on experimental findings reported in literature. We showed that graphene does not act as voids, instead it introduces randomly distributed porosities in the interfaces. These porosities are found to be the main reason behind the poor elastic and hardness properties of the nanocomposites.

2 MATERIAL AND METHOD

Bódis et al. [24] reported a change in mechanical properties of Si_3N_4 and graphene-Si_3N_4 nanocomposites that were manufactured via SPS using different sintering temperatures (1500 °C and 1600 °C) and holding times (3 min. and 10 min.). Tapasztó et al. [26] manufactured nanocomposites with the same SPS parameters (sintering temperatures and holding times). Those studies used multilayer graphene (MLG) or graphene nanoplatelets (GNPs) as reinforcement elements. Both stand for the same material, meaning they have got graphene stacks more than a few-layers and less than a graphitic sheet. Therefore, we combined microstructural and mechanical data given in those studies in order to create our finite element (FE) models. Kun et al reported thickness of multilayer graphene (MLG) as 10 nm [16]. Young's modulus of monolithic Si_3N_4, that is sintered at 1600 °C with 10 minutes of holding time, was given as 292 GPa in [24]. It was 233 GPa for 3 wt% graphene-Si_3N_4 nanocomposite under the same sintering conditions [24]. Tapasztó et al. [26] presented in their work a statistical orientation distribution of graphene nanoplatelets in Si_3N_4 matrix using scanning electron microscopy (SEM) images. Therefore, in order to obtain an approximately intermediate spatial distribution, three different representative volume elements (RVEs) were created based on random spatial distribution and the statistical distribution data given by Tapasztó et al. [26] (see Figure 1 (a), (b), (c)). Young's modulus of graphene and MLG (or GNP) was determined ~1 TPa by Lee et al. [10].

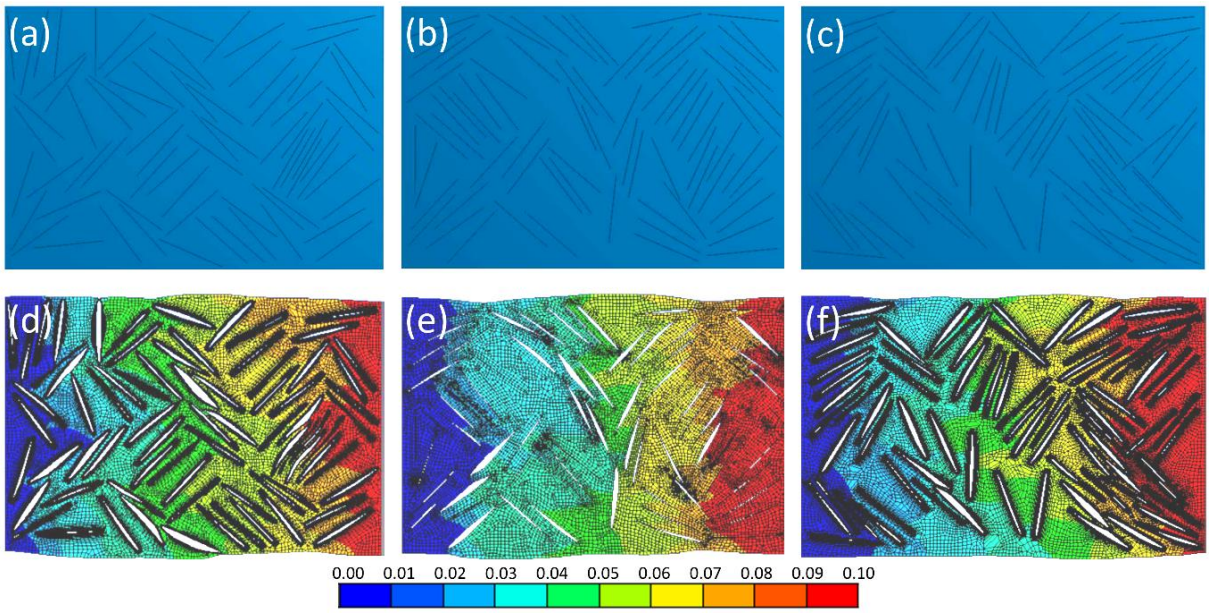

Figure 1. Three different RVE models (a,b,c) that were created based on the statistical distribution of graphene orientations. Each RVE is ~8µm by ~11µm. Respective FE models (d,e,f) that are strained by 0.1% (the legend bar shows axial strains in %). Deformation of the RVEs were scaled up by 10 in order to make voids more visible.

FE models were created in Hexagon Marc® Mentat software. The RVE models were built as ~8µm by ~11µm rectangle in order to approximate the SEM micrographs given by Tapasztó et al. [26]. Matrix phase was meshed with triangular (3-node) elements as its domain has got a complex geometry imposed by the dense and patternless distribution of graphene layers.Graphene layers, on the other hand, were meshed with quadrilateral (4-node) elements. Mechanical properties and element types defined on the models were given in Table 1. Boundary conditions were applied in a way to simulate a uniaxial tensile loading (see Figure 2). Nodes on the left edge of the RVEs were fixed horizontally (x-axis). One node that is about the mid of the left edge was also fixed vertically in order to avoid free body motion in y-axis. Nodes on the right were attached to a single node that is applied a displacement in x-axis. The displacement was applied as ~11nm, which makes a maximum strain of 0.001 (µm/µm).

Table 1. Mechanical properties and element types defined for the phases of the nanocomposites.

	Young's modulus	**Poisson's ratio**	**Element type**
Si_3N_4	292 GPa	0.28	Triangular element
Graphene	1 TPa	0.18	Quadrilateral element

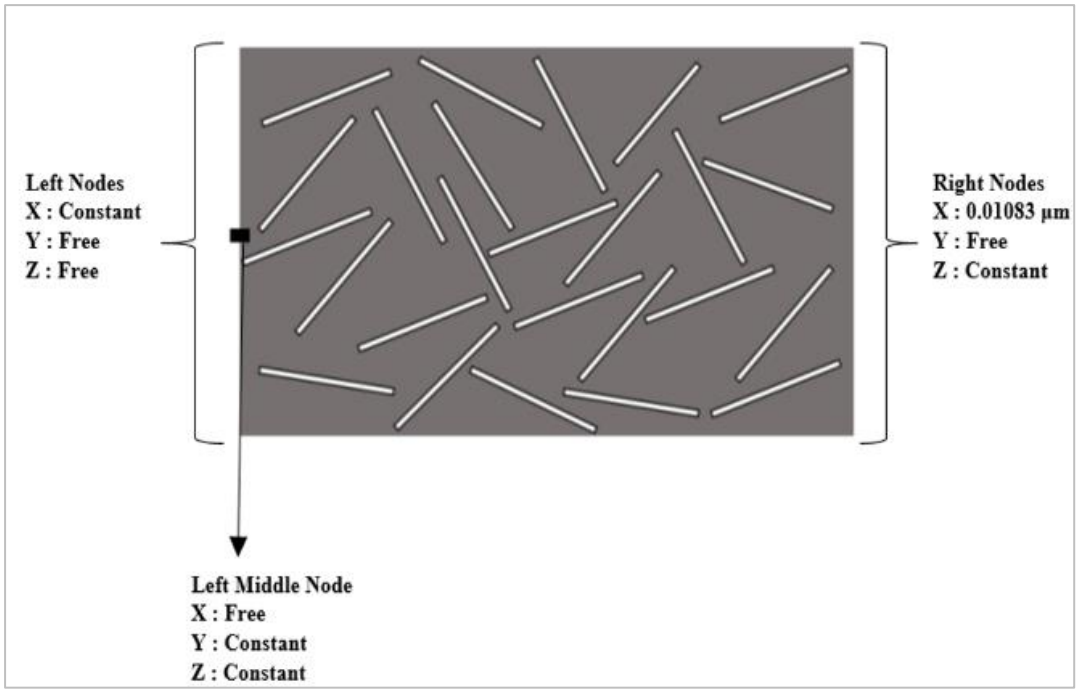

Figure 2. A schematical description of the boundary conditions applied on the FE models.

Three distinct interface scenarios were contemplated: graphene behaving as voids, graphene with no bonding to the Si_3N_4 matrix, and graphene with bonding to the Si_3N_4 matrix. The models with bonding applied were assigned varying bonding strength in order to observe how interfacial strength change affect the mechanical properties. All three RVE models (as shown in Figure 1(a), (b), (c) with graphene nanoplatelets assumed as voids were analyzed first. Displacement distributions of the analysis are given in Figure 1 (d), (e), (f)). Resulting Young's moduli of the models are given in Table 2. Among the three models, the RVE-b yielded an intermediate value and was hence chosen for further analyzes.

Table 2. Calculated Young's modulus of the RVE models with graphene acting as voids.

RVE models	Young's Modulus (GPa)
(a)	38.382
(b)	50.703
(c)	55.551

3 RESULTS AND DISCUSSION

Young's moduli of the RVE models with graphene acting as voids (vgRVE: void graphene RVE) were calculated as more than 4 times lower than that of the experimental results reported in the literature. Therefore, it is understood that graphene does not act as voids as some of the literature put forward [17], [19]. Second scenario where graphene nanoplatelets physically exist without making bonding with the surrounding matrix is assessed. In this, a touching contact was defined between the phases. Graphene was physically modelled in the second scenario (tgRVE: touching graphene RVE) as opposed to the first one where the areas that is normally occupied by the nanoplatelets were emptied out. Results of the second scenario was seen approximate to the first scenario. Only a slight increase in Young's modulus compared to the first scenario (an increase from 50.7 GPa to 52.2 GPa) was observed. Von Misses stress distributions are given in Figure 3. As can be seen in the Figure 3 (a) and (b), there is no significant differences between the stress distributions on the matrices of vgRVE and tgRVE models. Also, stresses induced on graphene nanoplatelets appeared to be smaller than those matrices, meaning graphene does not bear a considerable degree of load that comes onto the nanocomposites. These findings suggest that the mere presence of graphene is not sufficient for modeling the nanocomposites; there has to be a more profound interaction between the matrix and the reinforcement phase. For this reason, a third scenario was worked on.

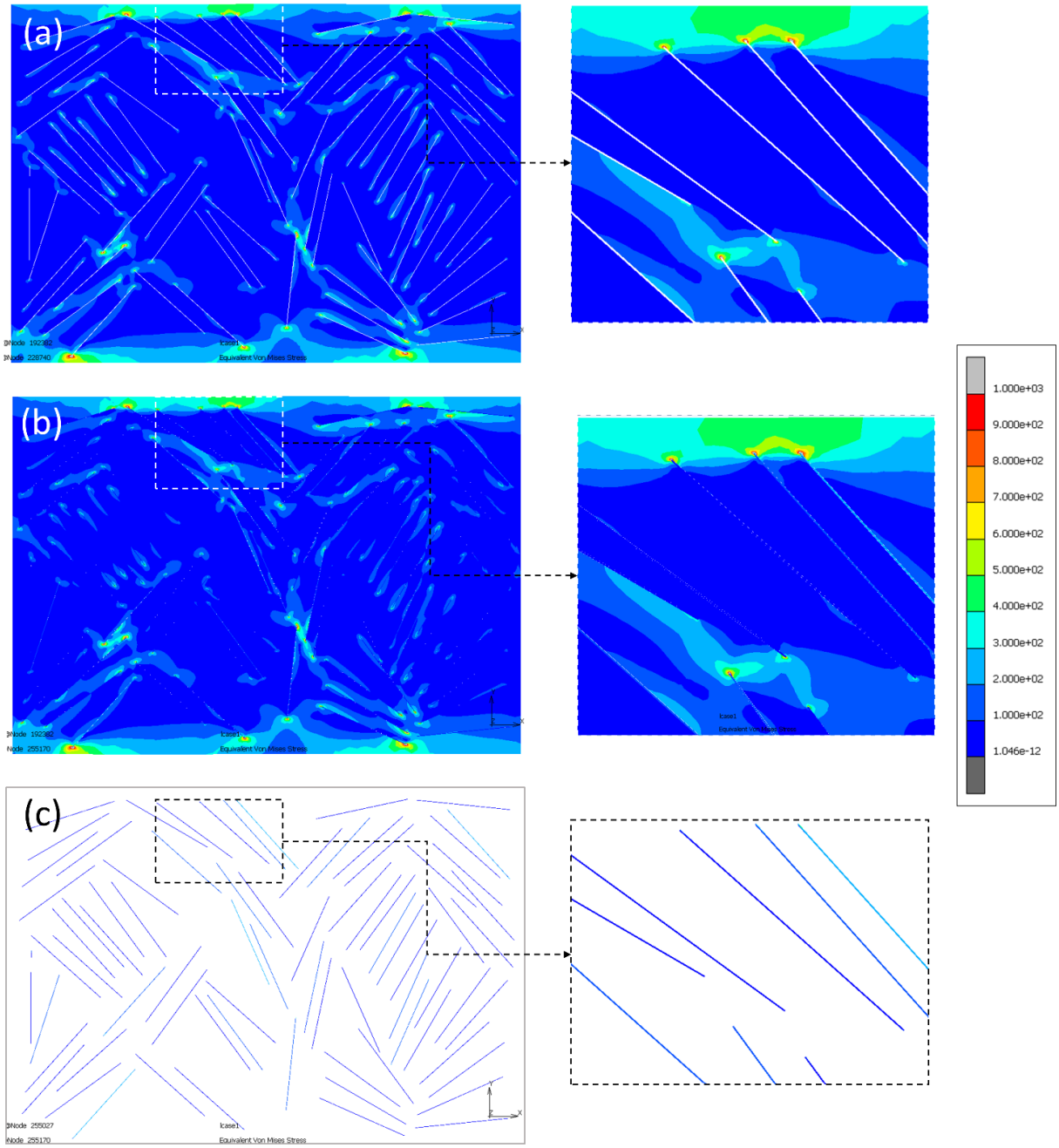

Figure 3. Von Misses stress distributions on matrix of (a) vgRVE, (b) tgRVE models. (c) Stress distributions on graphene nanoplatelets of tgRVE model. Detail images are given next to the main images. The scale bar shows stress in MPa and ranges from 1.046e-12 to 1000 MPa.

According to the third scenario, there is a continuous (glued) contact between the phases (ggRVE: glued graphene RVE). The contact was also assigned a stress limit, beyond which the glue contact was converted into a touching contact, leading to a weakened interface. No experimental data was yet provided in literature regarding the interfacial strength between graphene and Si_3N_4. The only closest data was reported by Li et al who described normal and

shear strength characteristics between graphene and boron nitride by employing molecular dynamics analysis [27]. From their study, normal and shear strength of the interfaces can be calculated as 350 MPa and 60 MPa, respectively. Here, we defined three different ggRVE models. All parameters, except the interfacial strength, are same in those models. In addition to the approximated values of 350 MPa and 60 MPa, smaller and larger values were assumed in order to see how the changes in interfacial strength affect the Young's modulus, toughness and stress distribution in the nanocomposites. The models and their corresponding interfacial strength values are given in Table 3.

Table 3. ggRVE models and their corresponding interfacial strength values.

ggRVE models	Interfacial normal strength (GPa)	Interfacial shear strength (GPa)
ggRVE1	234	40
ggRVE2	350	60
ggRVE3	467	80

Finite element simulations ggRVE models helped us study how interfacial strength affect the stress distribution in matrix and graphene nanocomposites. In addition, results of the simulations yielded a clue on the nature of distribution of porosities in the interfaces. An apparent change in the stress distribution in matrices was observed upon changing the interfacial strength. It can be seen in Figure 4 ((a), (b), (d), (e), (g), (h)) that degree of stress concentrations increases with increasing interfacial strength. In order to better analyze the stress distributions, one should assess the contact continuity (interface continuity) alongside. It can be seen from the contact continuity figures (Figure 4 (c), (f), (i)) that the nanoplatelets that have a continuous contact with the matrix experience more uniform stress distributions.

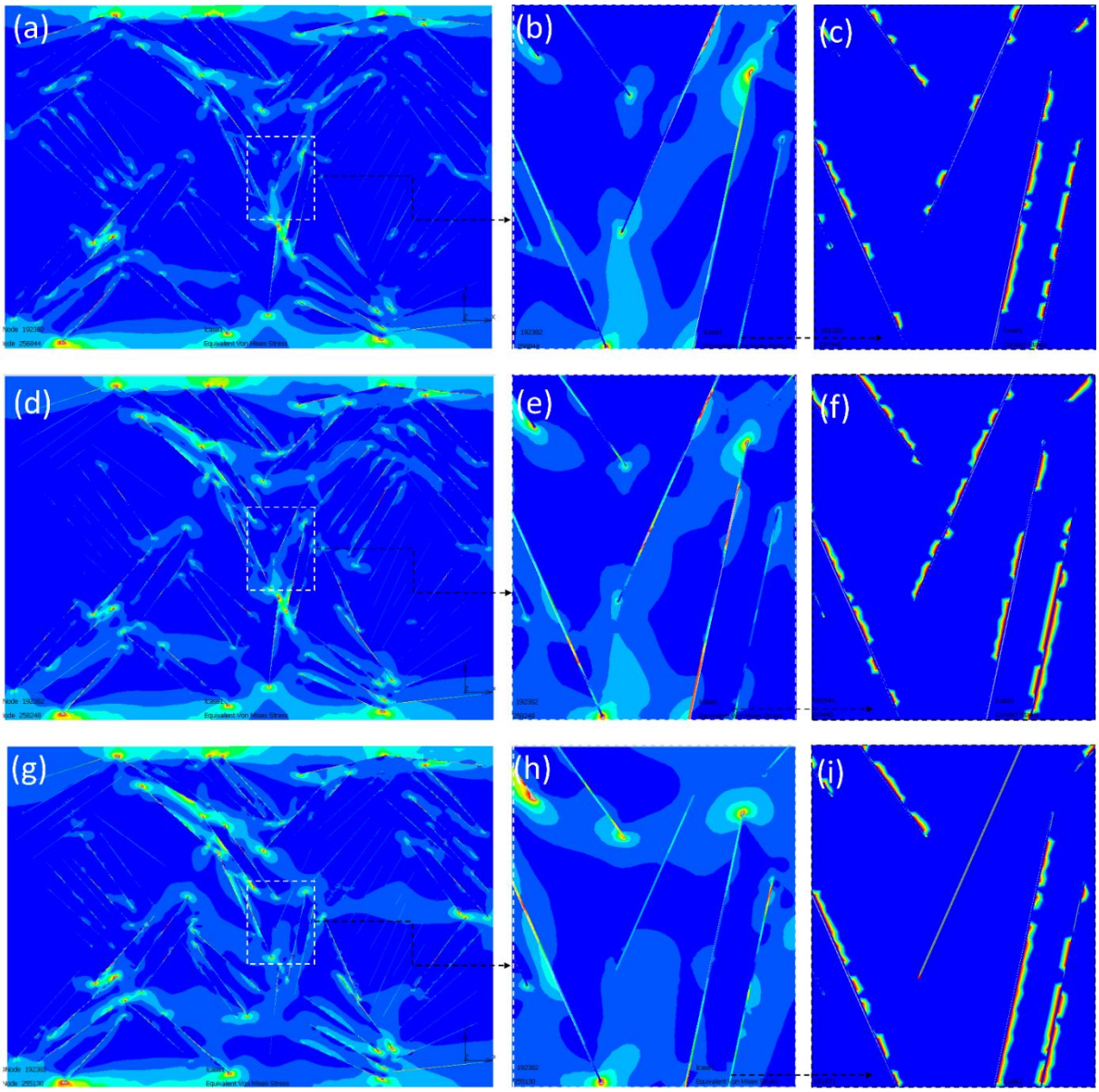

Figure 4. Von Misses stress distribution and contact continuity in ggRVE1 (a), ggRVE2 (d), ggRVE3 (g) models. Detail images ((b), (e), (h)) was provided right next to the full view of the nanocomposites. Contact continuity in the interfaces is shown in the rightmost images ((c), (f),(i)). (Refer to Figure 3 for colour scale legend).

Contact discontinuities observed in post-processing of ggRVE models (Figure 4 (c), (f), (I)) can be compared to the interfacial porosity phenomenon reported in literature [16], [18], [22], [24]. Stress-strain curves of the ggRVE models are given in Figure 5. Young's modulus of the models was calculated to be 302 GPa. No change in Young's modulus was observed, while an apparent trend in toughness improvement with increasing interfacial strength were seen. After bond breaking occur, smaller slopes in the curves, which emerged with the bond-breaking induced discontinuities (porosities), were obtained. Smaller slopes yielded a tangent

modulus of around 120 GPa. This means a smaller tangent modulus, therefore a smaller Young's modulus, is achievable in FE models upon introducing discontinuities (or porosities) into the interface of Si_3N_4 and graphene. Experimental results yielded a Young's modulus of nanocomposites much lower than the monolithic ceramic [24]. Therefore, by optimizing contact discontinuities, experimental Young's moduli of nanocomposites can be approximated more precisely.

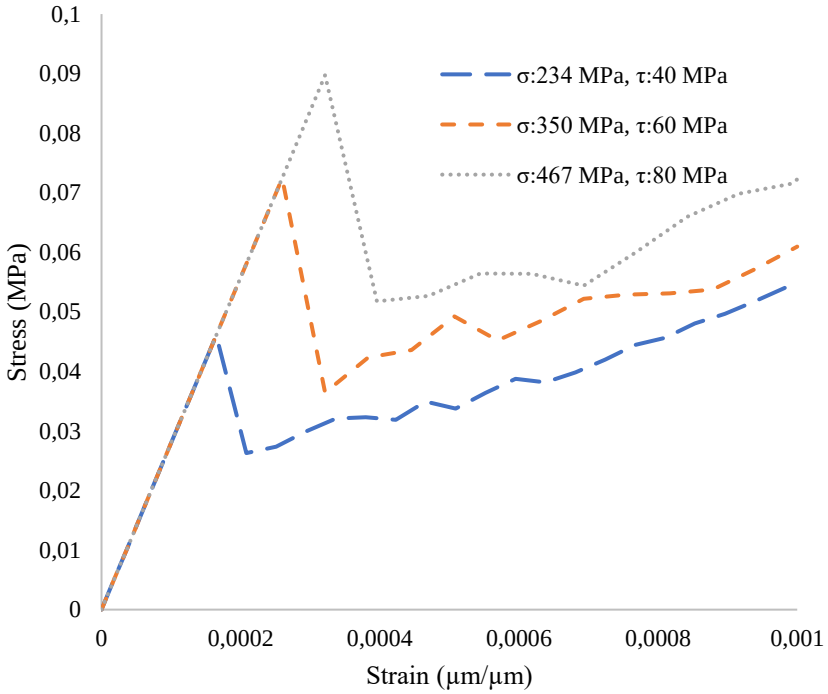

Figure 5. Stress-Stain curve of the ggRVE models of the nanocomposites with different interfacial strength values defined (σ: normal strength limit; τ: shear strength limit).

4 CONCLUSION AND SUGGESTIONS

Finite element models of graphene-Si_3N_4 nanocomposites were created based on microstructural data given in literature. The models were applied uniaxial tensile loading in order to study microstructural and mechanical characteristics of the nanocomposites. RVE models with different void, porosity, interfacial strength characteristics were examined. It was revealed that graphene does not behave like a void in the ceramic matrix. Instead, graphene introduces randomly distributed porosities in the interfaces, which was shown to influence the mechanical behavior of the nanocomposites significantly. Also, stress-strain curves and contact (interface) discontinuity analyze disclosed the primary reason behind the decrease of Young's modulus of the nanocomposites: Porosities in the interfaces decreases the slope (tangent

modulus) of the stress-strain curves. This observation suggests that graphene makes partial bonding with Si_3N_4, eventually leading to a reduction in Young's modulus of nanocomposites while simultaneously improving or at least maintaining the toughness.

Future studies are planned for developing more advanced finite element models that can simulate fracture mechanisms, including crack initiation, propagation, bridging, and pull out in graphene-reinforced Si_3N_4 nanocomposites. These future models will provide deeper insights into the failure behavior of the material and contribute to the design of more resilient nanocomposites. This study emphasizes the importance of optimizing interfacial porosity during the manufacturing stages. Future experimental studies should aim for methods that can control interfacial porosity distribution in order to obtain mechanically improved nanocomposites. In general, this study provides insights into understanding elastic behavior, interfacial interaction, and toughness characteristics of graphene-reinforced Si_3N_4 nanocomposites. By identifying the role of interfacial porosities in reducing Young's modulus of the nanocomposites, this study provides critical knowledge for future experimental and modeling studies.

Acknowledgements

We would like to acknowledge the generous support by BIAS Mühendislik Company for providing Marc Mentat software license along with other Hexagon Software packages.

Conflict of Interest Statement

There is no conflict of interest between the authors.

Statement of Research and Publication Ethics

The study is complied with research and publication ethics.

Artificial Intelligence (AI) Contribution Statement

This manuscript was entirely written, edited, analyzed, and prepared without the assistance of any artificial intelligence (AI) tools. All content, including text, data analysis, and figures, was solely generated by the authors.

REFERENCES

[1] F. Li *et al.*, "Ultrahigh piezoelectricity in ferroelectric ceramics by design," *Nat. Mater.*, vol. 17, no. 4, pp. 349–354, 2018, doi: 10.1038/s41563-018-0034-4.

[2] E. Vural, "Piston Malzemesi (AlSi12CuNi) Yüzeyine Uygulanmış Oksit Kaplamaların Termal Şok Testlerinin İncelenmesi," *Bitlis Eren Üniversitesi Fen Bilim. Derg.*, vol. 4, no. 1, Jul. 2015, doi: 10.17798/beufen.04292.

[3] C. Ramirez *et al.*, "Extraordinary toughening enhancement and flexural strength in Si3N4 composites using graphene sheets," *J. Eur. Ceram. Soc.*, vol. 34, no. 2, pp. 161–169, 2014, doi: 10.1016/j.jeurceramsoc.2013.08.039.

[4] R. B. Heimann, "Silicon nitride neramics: Structure, synthesis, properties, and biomedical applications," *Materials (Basel).*, vol. 16, no. 14, p. 5142, 2023, doi: 10.3390/ma16145142.

[5] H. Klemm, "Silicon nitride for high-temperature applications," *J. Am. Ceram. Soc.*, vol. 93, no. 6, pp. 1501–1522, 2010, doi: 10.1111/j.1551-2916.2010.03839.x.

[6] C. Ramírez, "10 Years of Research on Toughness Enhancement of Structural Ceramics By Graphene," *Philos. Trans. R. Soc. A Math. Phys. Eng. Sci.*, vol. 380, no. 2232, 2022, doi: 10.1098/rsta.2022.0006.

[7] G. Torğut, "Cevap Yüzey Yöntemi Kullanılarak Poli(VPi–ko-MA) / Grafen Kompozitlerinin İletkenliğinin Optimizasyonu," *Bitlis Eren Üniversitesi Fen Bilim. Derg.*, vol. 9, no. 1, pp. 36–44, Mar. 2020, doi: 10.17798/bitlisfen.563861.

[8] T. Mutuk and M. Gürbüz, "Fabricating Graphene-Titanium (<30μm) Composites by Powder Metallurgy Method: Microstructure and Mechanical Properties," *Düzce Üniversitesi Bilim ve Teknol. Derg.*, vol. 7, no. 2, pp. 89–97, Mar. 2019, doi: 10.29130/dubited.467622.

[9] A. K. Geim and K. S. Novoselov, "The rise of graphene," *Nat. Mater.*, vol. 6, no. 3, pp. 183–191, 2007.

[10] C. Lee, X. Wei, J. W. Kysar, and J. Hone, "Measurement of the elastic properties and intrinsic strength of monolayer graphene," *Science (80-.).*, vol. 321, no. 5887, pp. 385–388, 2008, doi: 10.1126/science.1157996.

[11] A. H. Castro Neto, F. Guinea, N. M. R. Peres, K. S. Novoselov, and A. K. Geim, "The electronic properties of graphene," *Rev. Mod. Phys.*, vol. 81, no. 1, pp. 109–162, 2009, doi: 10.1103/RevModPhys.81.109.

[12] O. Bayrak, M. Ionita, E. Demirci, and V. V. Silberschmidt, "Effect of morphological state of graphene on mechanical properties of nanocomposites," *J. Mater. Sci.*, vol. 51, no. 8, pp. 4037–4046, Apr. 2016, doi: 10.1007/s10853-016-9722-0.

[13] Y. Huang and C. Wan, "Controllable fabrication and multifunctional applications of graphene/ceramic composites," *J. Adv. Ceram.*, vol. 9, no. 3, pp. 271–291, 2020, doi: 10.1007/s40145-020-0376-7.

[14] J. Dusza *et al.*, "Microstructure and fracture toughness of Si 3N 4+graphene platelet composites," *J. Eur. Ceram. Soc.*, vol. 32, no. 12, pp. 3389–3397, 2012, doi: 10.1016/j.jeurceramsoc.2012.04.022.

[15] H. Seiner *et al.*, "Elastic properties of silicon nitride ceramics reinforced with graphene nanofillers," *Mater. Des.*, vol. 87, pp. 675–680, 2015, doi: 10.1016/j.matdes.2015.08.044.

[16] P. Kun, O. Tapasztó, F. Wéber, and C. Balázsi, "Determination of structural and mechanical properties of multilayer graphene added silicon nitride-based composites," *Ceram. Int.*, vol. 38, no. 1, pp. 211–216, 2012, doi: 10.1016/j.ceramint.2011.06.051.

[17] H. Seiner *et al.*, "Anisotropic elastic moduli and internal friction of graphene nanoplatelets/silicon nitride composites," *Compos. Sci. Technol.*, vol. 75, pp. 93–97, 2013, doi: 10.1016/j.compscitech.2012.12.003.

[18] M. Michálková, M. Kašiarová, P. Tatarko, J. Dusza, and P. Šajgalík, "Effect of homogenization treatment on the fracture behaviour of silicon nitride/graphene nanoplatelets composites," *J. Eur. Ceram. Soc.*, vol. 34, no. 14, pp. 3291–3299, 2014, doi: 10.1016/j.jeurceramsoc.2014.03.023.

[19] P. Rutkowski, L. Stobierski, D. Zientara, L. Jaworska, P. Klimczyk, and M. Urbanik, "The influence of the graphene additive on mechanical properties and wear of hot-pressed Si3N4 matrix composites," *J. Eur. Ceram. Soc.*, vol. 35, no. 1, pp. 87–94, 2015, doi: 10.1016/j.jeurceramsoc.2014.08.004.

[20] T. Cygan, J. Wozniak, M. Kostecki, B. Adamczyk-Cieslak, and A. Olszyna, "Influence of graphene addition and sintering temperature on physical properties of Si3N4 matrix composites," *Int. J. Refract.*

Met. Hard Mater., vol. 57, pp. 19–23, 2016, doi: 10.1016/j.ijrmhm.2016.02.003.

[21] C. Balázsi *et al.*, "Si3N4/graphene nanocomposites for tribological application in aqueous environments prepared by attritor milling and hot pressing," *J. Eur. Ceram. Soc.*, vol. 37, no. 12, pp. 3797–3804, 2017, doi: 10.1016/j.jeurceramsoc.2017.03.022.

[22] Y. Zhang, G. Xiao, M. Yi, and C. Xu, "Effect of graphene orientation on microstructure and mechanical properties of silicon nitride ceramics," *Process. Appl. Ceram.*, vol. 12, no. 1, pp. 27–35, 2018, doi: 10.2298/PAC1801027Z.

[23] O. Tapasztó *et al.*, "The effect of graphene nanoplatelet thickness on the fracture toughness of Si 3 N 4 composites," *Ceram. Int.*, vol. 45, no. 6, pp. 6858–6862, 2019, doi: 10.1016/j.ceramint.2018.12.180.

[24] E. Bódis *et al.*, "Toughening of silicon nitride ceramics by addition of multilayer graphene," *Ceram. Int.*, vol. 45, no. 4, pp. 4810–4816, 2019, doi: 10.1016/j.ceramint.2018.11.176.

[25] O. Bayrak, M. Tashkinov, V. V. Silberschmidt, and E. Demirci, "Quantitative analysis of orientation distribution of graphene platelets in nanocomposites using TEM," *Compos. Sci. Technol.*, vol. 262, p. 111084, Mar. 2025, doi: 10.1016/j.compscitech.2025.111084.

[26] O. Tapasztó *et al.*, "High orientation degree of graphene nanoplatelets in silicon nitride composites prepared by spark plasma sintering," *Ceram. Int.*, vol. 42, no. 1, pp. 1002–1006, 2016, doi: 10.1016/j.ceramint.2015.09.009.

[27] Y. Li, W. Zhang, B. Guo, and D. Datta, "Interlayer shear of nanomaterials : Graphene – graphene , boron nitride – boron nitride and graphene – boron nitride," *Acta Mech. Solida Sin.*, vol. 30, no. 3, pp. 234–240, 2017, doi: 10.1016/j.camss.2017.05.002.